GAS COMPRESSION MODERATES FLAME ACCELERATION IN DEFLAGRATION-TO-DETONATION TRANSITION

V. Bychkov*, D. Valiev*, V. Akkerman, and C.K. Law**,**
Vitaliy.bychkov@physics.umu.se
*Dept. Physics, Umeå University 901 87 Umeå, Sweden
**Dept. Mechanical and Aerospace Engineering, Princeton University, Princeton, NJ 08544-5263, USA

Abstract
We investigate the influence of gas compression on the developed stages of flame acceleration in smooth-wall and obstructed channels. We demonstrate analytically that gas compression moderates the acceleration rate. We also perform numerical simulations within the problem of flame transition to detonation. We show that flame acceleration undergoes three distinctive stages: 1) initial exponential acceleration in the incompressible regime, 2) gas compression moderates the process, so that the exponential acceleration regime goes over to a much slower one, 3) eventual saturation to a steady (or statistically-steady) high-speed deflagration velocity, which may be correlated with the Chapman-Jouguet deflagration speed. The possibility of deflagration-to-detonation transition is demonstrated.

Introduction

For a long time, deflagration-to-detonation transition (DDT) remained one of the least understood processes of hydrodynamics and combustion science in spite of its extreme importance. During the process, a usual slow flame accelerates spontaneously with velocity increase by 3 orders of magnitude until an explosion occurs and develops into a self-sustained detonation [1-8]. The first qualitative explanation of the flame acceleration in tubes with slip walls has been suggested by Shelkin in 40-ies [2]. The Shelkin mechanism involved thermal expansion of the burning gas, non-slip at the tube walls and turbulence as the main components of flame acceleration. When a flame propagates from a closed tube end, the burning gas expands and pushes a flow of the fuel mixture, see Fig. 1. The flow becomes strongly non-uniform because of non-slip at the walls. The non-uniform velocity distribution makes the flame shape curved, which increases the burning rate and drives the acceleration. Turbulence provides additional distortion of the flame front and compensates for thermal losses to the walls. Acceleration of turbulent flames was observed in numerous experiments [3-7], still, for a long time there was almost no progress in the quantitative theoretical understanding of the process because of the complications related to turbulent burning. Despite a century of intensive research, turbulence in general and turbulent burning in particular belong to the most difficult problems of modern physics.

Considerable progress in understanding the flame acceleration started recently within the approach of a laminar flow with the direct numerical simulations and the analytical theory supporting each other. The analytical theory of laminar flame acceleration in smooth tubes has been developed and validated by extensive numerical simulations in Refs. [9-11]. In tubes with obstacles, Bychkov et al. [12,13] identified a new ultra-fast mechanism of flame acceleration, which is much stronger than the classical Shelkin scenario. By use of analytical theory and numerical simulations, papers [12,13] demonstrated that delayed burning between the obstacles creates a powerful jet-flow, driving the acceleration. The new mechanism is independent of the Reynolds number, with turbulence playing only a supplementary role. Still, in both configurations of smooth-wall and obstructed tubes (channels), the theory of flame acceleration [9-13] employed the limit of an incompressible flow, which holds with a good accuracy at the beginning of the process. For example, a typical value of the unstretched

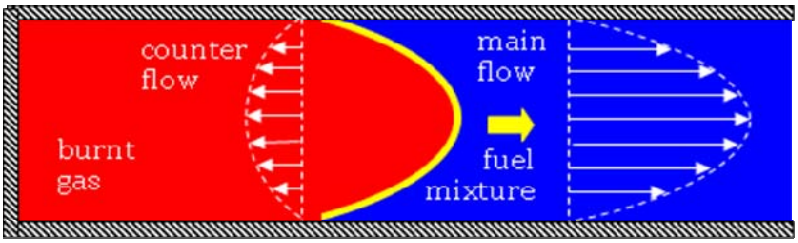

Figure 1. Schematic of the Shelkin mechanism of flame acceleration and the influence of gas compression.

laminar flame velocity U_f for hydrocarbon flames is about 40 cm/s, which is much smaller than the sound speed c_s in the fuel mixture. Initial values of the Mach number related to flame propagation are quite small $Ma \equiv U_f / c_s \cong 10^{-3}$, hence the effects of gas compression may be neglected at the beginning of the process. The theories [9-13] predicted fast initial acceleration of laminar flames in micro-scale tubes in the exponential regime. Recent experiments in ethylene-oxygen mixtures [14] confirmed the possibility of flame acceleration and DDT in micro-tubes with diameters about 1 mm. At the same time, the experiments [14] demonstrated a number of specific effects beyond the scope of the incompressible flow models [9-13]; e.g. the saturation of the flame velocity to a steady value below the Chapman-Jouguet (CJ) detonation speed. The saturation velocity can be interpreted as the CJ deflagration speed [1], which is subsonic with respect to the fuel mixture just ahead of the flame front and supersonic in the reference frame of the tube walls. Similar saturation of the flame propagation speed to a supersonic value with respect to an observer has been detected experimentally in channels with obstacles; this regime is often called "fast flames" [4,5]. In order to explain these effects, one has to account for gas compression in both geometries of smooth tubes and tubes with obstacles.

In this report, we investigate the influence of gas compression on flame acceleration at the developed stages in both geometries. We demonstrate analytically that gas compression moderates the acceleration rate. We also perform direct numerical simulations within the problem of flame transition to detonation. We show that flame acceleration undergoes three distinctive stages: 1) initial exponential acceleration in the incompressible regime, 2) gas compression moderates the process; consequently, the exponential acceleration regime goes over to a much slower one, 3) eventual saturation to a steady high-speed deflagration velocity. The saturation velocity of deflagration may be correlated with the CJ deflagration speed. The possibility of DDT is demonstrated.

The role of gas compression in moderating flame acceleration in smooth tubes

Figure 1 illustrates schematically the Shelkin mechanism of flame acceleration in tubes with smooth walls, as well as the moderating role of gas compression in the process. At the incompressible stage, burning involves decrease of the gas density by a factor $\Theta \equiv \rho_f / \rho_b$, which is typically rather large. For the burning rate U_w (roughly, the laminar flame speed U_f multiplied by a scaled increase in the flame surface area due to curvature), the flame front produces the extra volume of the gas $(\Theta - 1)U_w$ per unit time. At the initial incompressible stage of flame acceleration, the burnt gas is mostly at rest due to the boundary conditions at the closed tube end, so that the extra volume results in a flow of the fuel mixture only. Accounting for gas compression, we obtain a counter-flow in the burnt matter in addition to the main flow in the fuel mixture. Initially, the role of the counter-flow is as small as

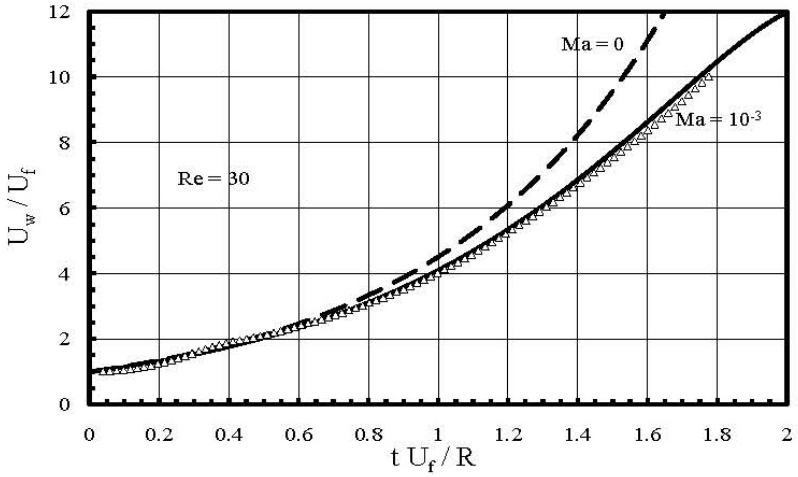

Figure 2. Scaled burning rate for $\Theta = 8$, $\gamma = 1.4$, Re = 30 as predicted by the theory for $Ma = 0; 10^{-3}$ (lines) and found in numerical simulations (markers).

$Ma << 1$, but it increases as the flame accelerates. Quantitative theory of the flame acceleration in a smooth 2D channel of half-width R has been developed in Ref. [15] considering influence of gas compression as Taylor series for a small parameter $Ma << 1$. According to Ref. [15], the velocity $\dot{Z}_f$, found for the average position $Z_f(t) = \langle z_f(x,t) \rangle$ of the elongated flame front $z = z_f(x,t)$, obeys the differential equation

$$\ddot{Z}_f = \frac{U_f}{R}\sigma \dot{Z}_f \left(1 - MaB\frac{\dot{Z}_f}{U_f}\right), \tag{1}$$

where the scaled rate σ,

$$\sigma = \frac{(\mathrm{Re}-1)^2}{\mathrm{Re}}\left(\sqrt{1+\frac{4\,\mathrm{Re}\,\Theta}{(\mathrm{Re}-1)^2}}-1\right)^2, \tag{2}$$

characterizes exponential acceleration at the initial incompressible stage, $\dot{Z}_f \propto U_f \exp(\sigma U_f t / R)$, as found in Ref. [9], $\mathrm{Re} = U_f R/\nu$ plays the role of the Reynolds number related to a planar flame, B is a numerical factor found in Ref. [15] as

$$B = \frac{\Theta - 1}{\Theta}\left[(\gamma - 1)\frac{\Theta - 1}{\Theta} + 1\right]\frac{1+S}{1-(\Theta-1)S},$$

γ is the adiabatic exponent, and the designation S stands for

$$S = \frac{\sqrt{\sigma\,\mathrm{Re}}}{(\sqrt{2\sigma\,\mathrm{Re}}-1)(\sqrt{\sigma\,\mathrm{Re}}+\sqrt{2}\sigma)}.$$

As described by Eq. (1), the flame accelerates in the exponential regime at the initial stage, as long as the front velocity is sufficiently low in comparison with the sound speed, $\dot{Z}_f / c_s << 1$. As the flame velocity approaches the sound speed, the role of gas compression (expressed by the term $\propto Ma\dot{Z}_f / U_f$) increases and thereby moderates the acceleration regime. Qualitatively, the solution to Eq. (1) describes the transition from the initial exponential regime of flame acceleration to almost linear acceleration and then to saturation of the flame velocity as

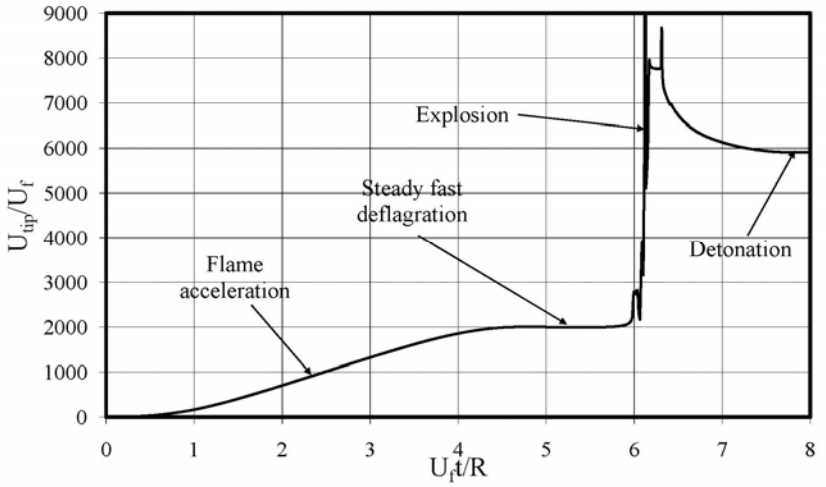

Figure 3. Evolution of the flame tip velocity for $\Theta = 8$, $\gamma = 1.4$, $\mathrm{Re} = 6.7$, $Ma = 10^{-3}$ until the full-developed CJ detonation.

$$\dot{Z}_f / U_f = \frac{\Theta \exp(\sigma U_f t / R)}{1 + MaB\Theta \exp(\sigma U_f t / R)}, \qquad (3)$$

However, quantitatively, Eqs. (1), (3) hold only as long as the term $MaB\Theta \exp(\sigma U_f t / R) << 1$ is small and may be treated as a correction in Taylor series. Figure 2 compares the analytical theory Eqs. (1), (3) to the numerical simulations of Ref. [9]; we find good agreement of the theory and the simulations as long as the flame speed is relatively small.

The role of gas compression at the developed stages of flame acceleration has been demonstrated in Ref. [16] using direct numerical simulations. Figure 3 presents the tip velocity of the reaction front versus time for $\mathrm{Re} = 6.7$, $Ma = 10^{-3}$ and $\Theta = 8$; the plot demonstrates all elements of the DDT from initial flame acceleration to steady detonation. Focusing at the acceleration process, we observe several different stages: 1) initially, the flame accelerates exponentially in an isobaric (incompressible) regime; 2) later, the acceleration regime moderates to approximately linear velocity increase; 3) subsequently, the flame velocity saturates to the quasi-steady regime with supersonic velocities in the laboratory reference frame. The saturation velocity is comparable to the CJ deflagration speed. Quite often, we find saturation process in the form of two steps, which is, presumably, related to viscous stress at the channel walls. The effect of gas compression, both behind the flame front and ahead of the front, can be observed directly in Fig. 4, which presents the density and velocity profiles along the channel axis at various time instants. Compression of the burnt gas behind the front is relatively uniform in agreement with the theory [15]. In contrast, in the fresh fuel mixture we can see a non-uniform adiabatic compression wave and a shock pushed by the flame. When the flame tip reaches the distance about $Z_{tip} \cong 3 \cdot 10^3 R$ from the closed end of the channel, the density of the fuel mixture in the compression wave exceeds its initial value approximately 3-4 times. Maximal possible gas compression that could be achieved in a shock wave is $(\gamma+1)/(\gamma-1)$, see Ref. [1], which equals 6 in the present case. Velocity distribution in Fig. 4 shows also the region of the counter-flow (negative velocity) behind the flame front, which tends to moderate the acceleration.

We also demonstrate that the flame acceleration leads finally to detonation triggering. The whole multi-dimensional picture of the final stage of the DDT is shown in Fig. 5 with color representation for temperature. Figure 5 (a) shows all elements of flame dynamics at that

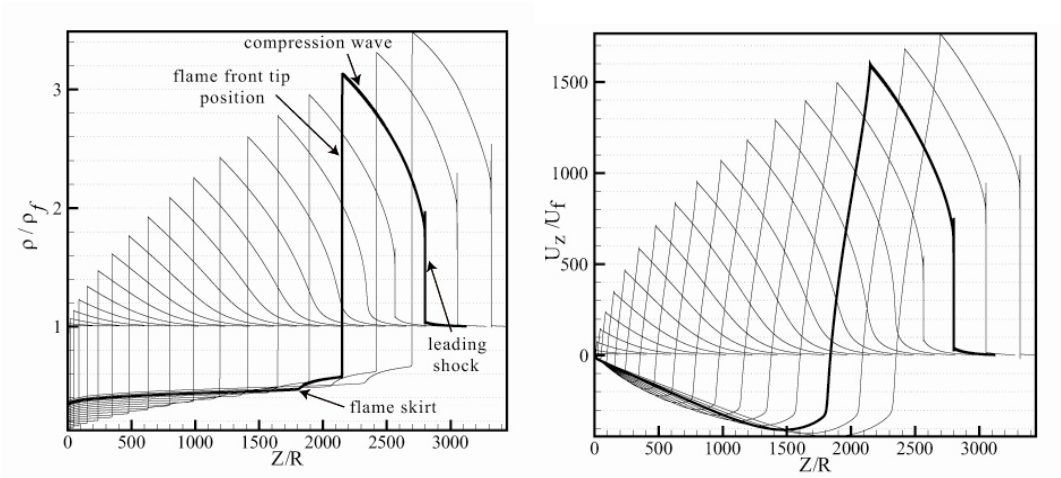

Figure 4. Density and velocity profiles along the channel axis for $\mathrm{Re} = 6.7$. Time instants are equally spaced in the range of $(0-3.8)U_f t/R$. The plot selected by bold is related to $U_f t/R = 3.28$.

stage, figures (b) and (c) illustrate some interesting features of the process in detail. In Fig. 5 (a) we squeeze the pictures in z-direction to make the whole flow structure visible (we remind that the channel width is 2*R*). The central part in the first snapshot shows the elongated flame front at the very beginning of the explosion. In addition, we can see the explosion starting along the walls because of viscous heating as explained in Ref. [16]. The process is more pronounced in the second snapshot. Tongues of the explosion burst along the walls at high speed, catch up with the flame tip (second snapshot) and then leave it far behind engulfing the flame (third snapshot). Interaction of the explosion and the flame produces a strong turbulent flow, which enhances burning. Figures 5 (b) and (c) indicate that turbulence develops as a result of hydrodynamic instabilities. Presumably, these are the Kelvin-Helmholtz, Rayleigh-Taylor and Richtmyer-Meshkov instabilities. We can recognize classical elements of the instabilities: small perturbations at the beginning in Fig. 5 (b), a vortex street, "cat-eye" vortices and the "mushroom"-shape of the leading part of the flame front in Fig. 5 (c). Configuration of the turbulent burning region resembles the characteristic shape of an accelerating turbulent flame observed in the experiments [4,5] quite well. Experimental papers typically describe the process as fast turbulent burning in a boundary layer, which pushes a strong shock thereby reducing the reaction time in the fuel mixture and facilitating the explosion. Since the shock is almost planar, the explosion spreads from the channel walls to the axis and produces detonation considerably ahead of the turbulent flame brush. Again, we emphasize strong resemblance between the present simulations and the scenario of "explosion-within-explosion" well-known from the experimental works [4]. A large pocket of unburnt gas remains trapped behind the detonation front. The detonation is seen on the last snapshot of Fig. 5 (a).

Gas compression moderates flame acceleration in tubes with obstacles

As demonstrated in Refs. [12,13], the physical mechanism of flame acceleration in obstructed tubes/channels differs qualitatively different from the classical Shelkin mechanism [9,10]. This new mechanism is extremely strong, providing flame acceleration that is independent of the Reynolds number, and as such may be quite important for technical applications. Specifically, fast flame propagation in the free central part of an obstructed channel creates pockets of fresh fuel mixture between the obstacles, as illustrated in Fig. 6. Gas expansion due

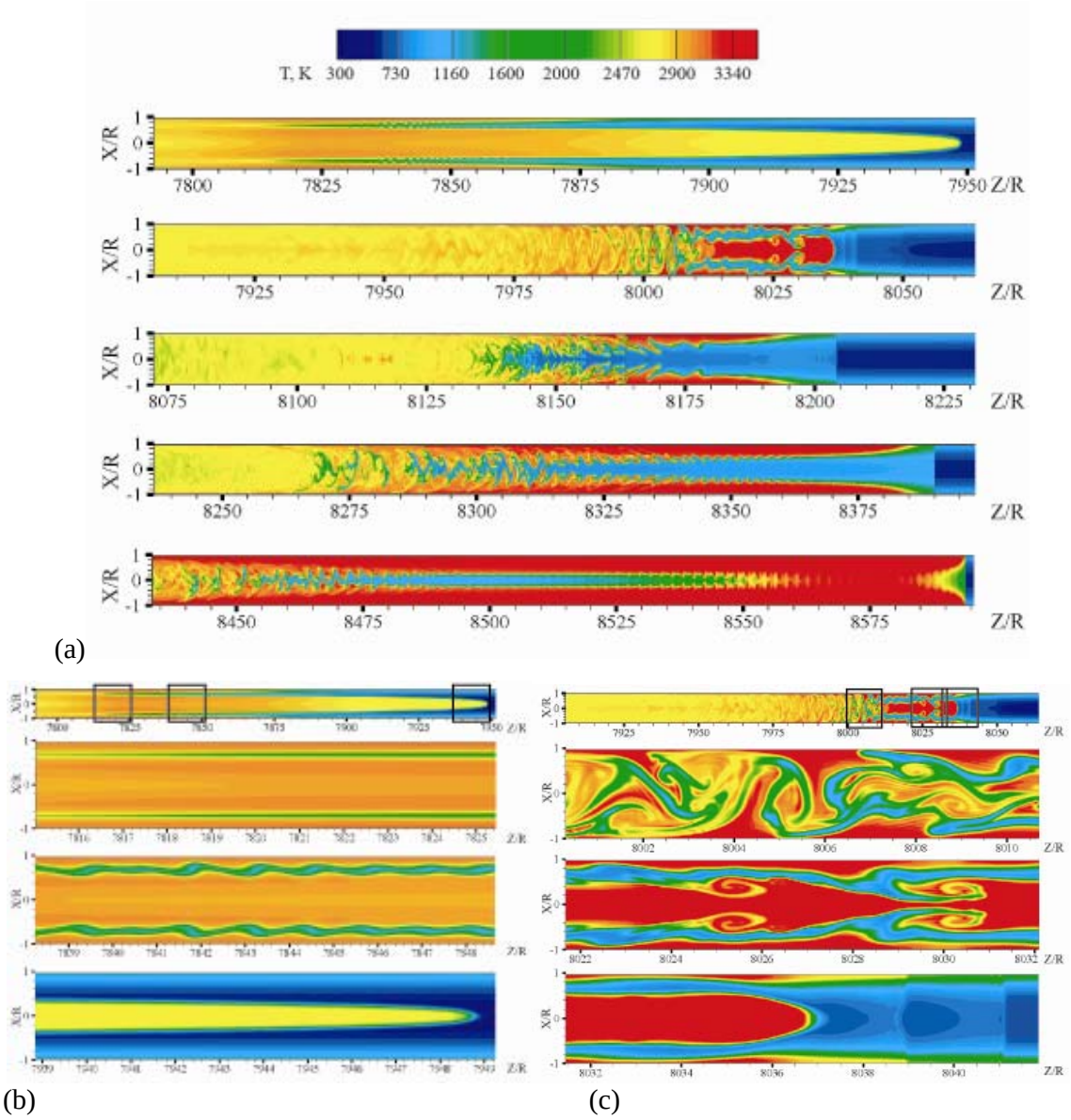

Figure 5. Temperature field during DDT for $\mathrm{Re} = 10$; (a) Time instants are equally spaced in the range $(7.0 - 7.16)U_f t / R$; (b) Close-up view with original aspect ratio on time instant $7.0U_f t / R$; (c) Close-up view on time instant $7.04U_f t / R$.

to delayed burning in the pockets produces a powerful jet flow in the unobstructed part of the channel. The jet flow renders the flame tip to propagate even faster, which produces new pockets, generates a positive feedback between the flame and the flow, and leads to flame acceleration. According to the theory [12] developed within the limit of incompressible flow, propagation of the flame tip is described by the equation

$$\dot{Z}_{tip} = \frac{(\Theta - 1)U_f}{(1-\alpha)R} Z_{tip} + \Theta U_f , \qquad (4)$$

which implies exponential acceleration $\dot{Z}_{tip} \propto \exp(\sigma U_f t / R)$ with the scaled acceleration rate $\sigma_0 = (\Theta - 1)/(1-\alpha)$ independent of the Reynolds number. Similar to smooth tubes, flame

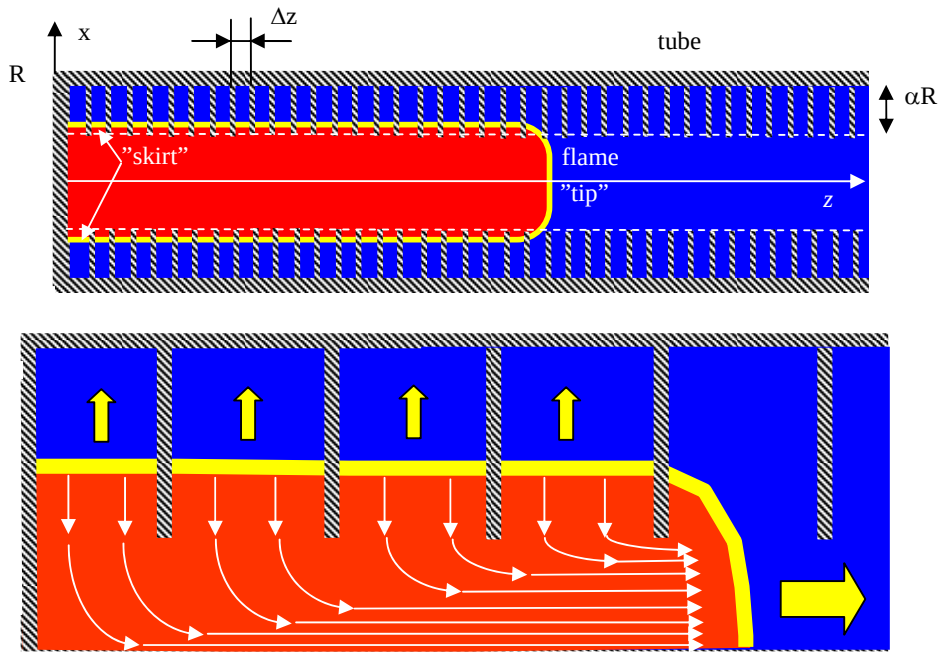

Figure 6. Schematic of the physical mechanism of flame acceleration in tubes with obstacles.

acceleration occurs because of the extra gas volume produced in the burning process and indicated by the factor $(\Theta-1)$ in Eq. (4). As long as gas compression is negligible (at the initial stage of flame acceleration), this extra volume results in the jet flow shown in Fig. 6. However, as the speed of the flame tip approaches the sound speed, the effects of gas compression become important; they make the jet flow in Fig. 6 weaker and moderate the acceleration process. The quantitative theory of the moderation mechanism has been developed in Ref. [17] using the Taylor series for $Ma << 1$. Accounting for small, but finite gas compression we can extend the theoretical results Ref. [12] to

$$\dot{Z}_{tip} = \sigma_1 Z_{tip} - Ma\frac{\sigma_0^2}{U_f}\left(\frac{1}{1-\alpha}+\gamma-1\right)Z_{tip}^2 + \Theta\left(1-Ma(\gamma-1)\frac{(\Theta-1)^2}{\Theta}\right)U_f, \qquad (5)$$

with the designation

$$\sigma_1 = \sigma_0\left[1-Ma\left(\frac{\Theta}{1-\alpha}+2(\gamma-1)(\Theta-1)\right)\right].$$

Similar to Eq. (1) for tubes with smooth walls, the derived equation (5) describes moderating influence of gas compression in tubes with obstacles. The moderating role is incorporated both in linear and nonlinear terms in Z_{tip}. Figure 7 compares the analytical results obtained for the incompressible flow, Eq. (4), the weakly compressible flow, Eq. (5), and the numerical data of Refs. [12,13]. In all three cases, the theory developed for non-zero Mach numbers agrees well with the simulation results at the initial stage of flame acceleration, but deviates at later stages. The states of deviation approximately correspond to the same level of flow compressibility, $u_z / c_s \approx 0.1$, which is achieved faster for larger values of the blockage ratio, e.g. at $Z_{tip}/R \approx 4.4; 6.6; 8.8$ for $\alpha = 1/3; 1/2; 2/3$, respectively. Still, the flame accelerates extremely fast in channels with obstacles, which makes validity of the formulation based on the Taylor series quite limited in time.

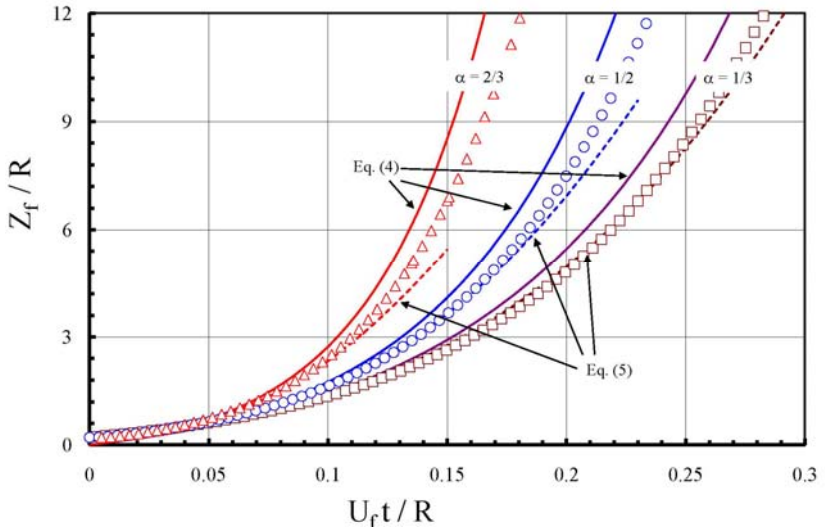

Figure 7. Flame tip position for $\Theta = 8$, $\gamma = 1.4$ as predicted by the theory for $Ma = 0; 10^{-3}$ and different values of the blockage ratio $\alpha = 1/3; 1/2; 2/3$ (lines), and found in the numerical simulations (markers).

In order to study the role of gas compression at the developed stages of flame acceleration in obstructed channels, we performed direct numerical simulations of the Navier-Stokes combustion equations. Characteristic temperature and velocity distribution at the initial stage of the process are shown in Fig. 8, where we easily recognize the main elements of the new acceleration mechanism, namely, fast spreading of the flame fronts in the central free part of the channel, delayed burning in the pockets and the strong jet flow. Figure 9 shows position of the flame tip versus time (scaled according to Eq. (4)) as predicted by the theoretical model of incompressible flow and found in numerical simulations for different initial values of the Mach number. As we can see, the limit of incompressible flow holds with good accuracy for $Ma = 10^{-3}$; still, deviations are noticeable already for $Ma = 5 \cdot 10^{-3}$. For $Ma = 10^{-2}$ the deviations are even stronger with the effective acceleration rate smaller by a factor of about 2 as compared to the predictions of Eq. (4). Still, all plots of Fig. 9 demonstrate almost exponential acceleration of the flame tip versus time, which correspond to

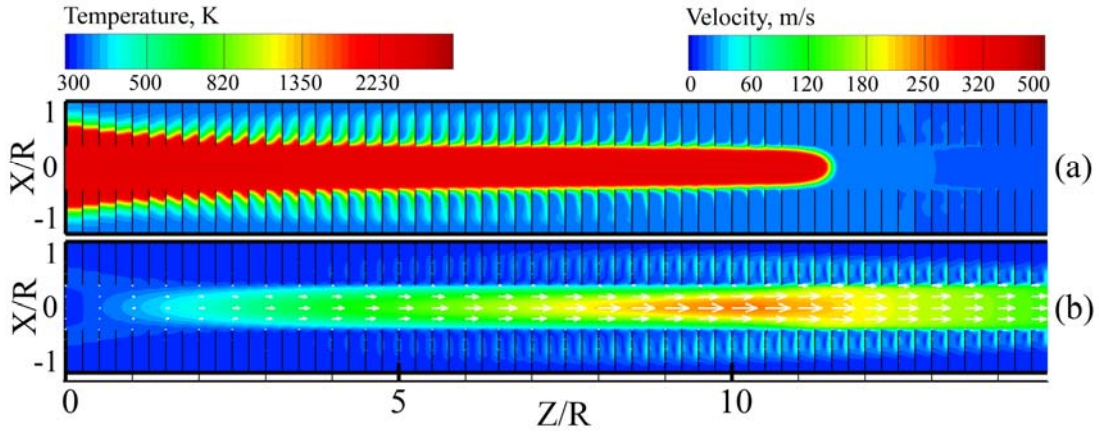

Figure 8. Snapshots of temperature (a) and velocity (b) of burning in channels with obstacles for $\Theta = 8$, $Ma = 10^{-3}$, $\alpha = 2/3$, $\Delta z / R = 1/4$.

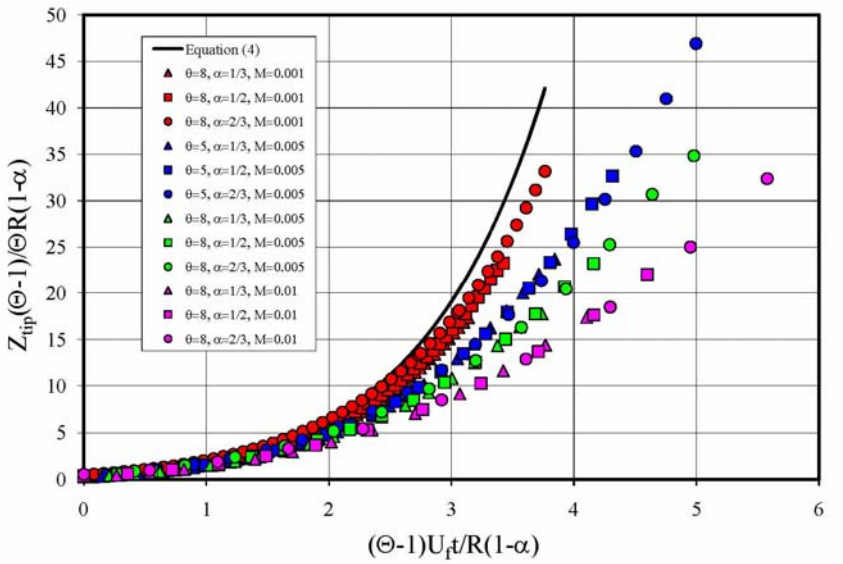

Figure 9. Flame tip position as predicted by the theory for $Ma = 0$ and obtained in the simulations for different values of the blockage ratio $\alpha = 1/3; 1/2; 2/3$, $\Theta = 5; 8$ and $Ma = 10^{-3}; 5\cdot 10^{-3}; 10^{-2}$ (markers).

the relatively initial stage of flame acceleration. Modification of the acceleration regime occurs at later stages of the process as presented in Fig. 10. The moderation of flame acceleration because of gas compression agrees with the concept that the flame propagation velocity cannot exceed the limiting value of the CJ deflagration speed, for which the downstream flow is sonic. We therefore expect saturation of the flame tip velocity to a certain steady value at the end of the acceleration process, but prior to an explosion. Indeed, Fig. 10 demonstrates such saturation, obtained computationally at the final stage of flame acceleration, for various blockage ratios.

Finally, we discuss how flame acceleration in obstructed channels may lead to DDT. It is well known that any flame propagating from a closed end pushes a flow in the fuel mixture with a weak shock/compression wave at the head of the flow. The flame acceleration renders the compression wave stronger, until it develops into a shock of considerable amplitude. Preheating of the fuel mixture by the shock is conventionally considered as one of the main elements of DDT both in obstructed and unobstructed tubes/channels [2-4]. The temperature behind the shock increases, and the reaction time in any compressed gas parcel decreases drastically. The decrease in the reaction time may result in explosion and DDT ahead of the flame front unless the parcel is burnt by the flame before active explosion is initiated. Thus, in general, we may expect two possible outcomes for the flame acceleration: 1) if the reaction time behind the shock is sufficiently short, then it drives the explosion and DDT; 2) the reaction time may be longer than the interval available for a gas parcel to travel between the shock and the flame. In the latter case, explosion does not occur and the final state of flame acceleration is the CJ deflagration. Both CJ detonation and deflagration have been experimentally found in smooth tubes [14]. In the numerical simulations for the geometry of obstructed channels, we also observed both possibilities of DDT and CJ deflagration for different reaction kinetics. Taking reaction of the first order with respect to density (designated by $n = 1$ in Fig. 10), we obtained statistically steady CJ deflagration at the end of flame acceleration with no explosion or DDT. This result indicates that the decrease in the reaction time behind the shock is not sufficient, and the gas parcels are consumed by the flame front before spontaneous reaction develops into a powerful explosion. Thus, in order to

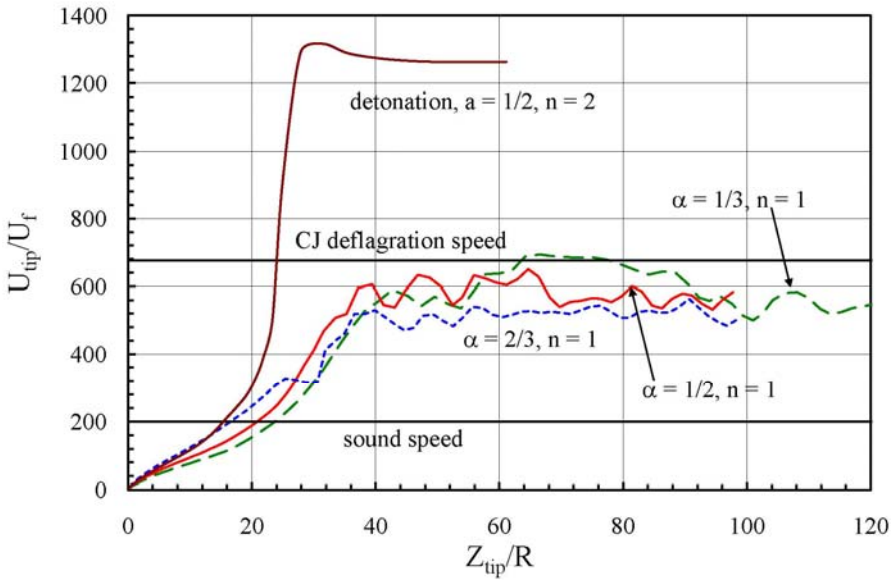

Figure 10. Time dependence of the flame tip velocity for $\Theta = 8$, $\alpha = 1/3; 1/2; 2/3$, $Ma = 5 \cdot 10^{-3}$ and different reaction order with respect to density $n = 1; 2$.

observe DDT, we needed to take another reaction mechanism, e.g. with $n = 2$, which is more sensitive to pressure and temperature increase in the shock, and obtained explosion triggering and DDT, see Fig. 10. Remarkably, in this case the reaction rate is so sensitive to pressure and temperature that the DDT occurs before the flame reaches the CJ deflagration state.

Summary

In this presentation, we considered the role of gas compression in moderating flame acceleration in DDT. Both geometries of channels with smooth walls and with obstacles have been considered. Previous theoretical results [9-13] have been limited to the initial acceleration stage in the incompressible flow, which results in an exponential regime of flame acceleration. Accounting for first-order terms in the Taylor series for small, but finite Mach number, we demonstrate that gas compression modifies the exponential regime into a much slower one. The developed stages of flame acceleration with considerable gas compression have been studied using direct numerical modeling, which substantiates predictions of the analytical theory and shows moderation of the acceleration regime and eventual saturation to steady (or statistically-steady) fast flame propagation, which can be associated with the CJ deflagration known from the classical theory [1]. We also demonstrate the possibility of DDT both for channels with smooth walls and with obstacles.

Acknowledgements

This work was mostly supported by the Swedish Research Council (VR) and the Swedish Kempe Foundation. The numerical simulation was performed at the High Performance Computer Center North (HPC2N), Umea, Sweden. The work at Princeton University was supported by the US Air Force Office of Scientific Research.

References

[1] Landau, L.D., Lifshitz, E.M., *Fluid Mechanics*, Pergamon Press, Oxford 1989.
[2] Shelkin, K., *J. Exp. Teor. Phys*. 10: 823 (1940).
[3] Roy, G.D., Frolov, S.M., Borisov, A.A., Netzer, D.W., *Prog. En. Combust. Sci.* 30: 545 (2004).
[4] Ciccarelli G., Dorofeev S., *Prog. En. Combust. Sci.* 34: 499 (2008).
[5] Kuznetsov, M., Alekseev, V., Matsukov, I., Dorofeev, S., *Shock Waves* 14: 205 (2005).
[6] Frolov, S. , Semenov, I., Utkin, P., Komissarov, P., Markov, V., *Proceedings of 21st ICDERS*, Poitiers, France 2007, paper 215.
[7] Johansen C. and Ciccarelli, G., *Combust. Flame* 156: 405 (2009).
[8] Gamezo, V., Ogawa, T., Oran, E., *Combust. Flame* 155: 302 (2008).
[9] Bychkov, V., Petchenko, A., Akkerman, V., Eriksson, L.-E., *Phys. Rev. E* 72: 046307 (2005).
[10] Akkerman, V., Bychkov, V., Petchenko, A., Eriksson, L.-E., *Combust. Flame* 145: 206 (2006).
[11] Bychkov, V., Akkerman, V., Fru, G., Petchenko, A., Eriksson, L.-E., *Combust. Flame* 150: 263 (2007).
[12] Bychkov, V., Valiev, D., Eriksson, L.-E., *Phys. Rev. Lett.* 101: 164501 (2008).
[13] Valiev, D., Bychkov, V., Akkerman V., Law C.K., Eriksson, L.-E., *Combust. Flame* 157: 1012 (2010).
[14] Wu, M., Burke, M., Son S., Yetter R., *Proc. Combust. Inst.* 31: 2429 (2007).
[15] Bychkov V., Akkerman V., Valiev D., Law C.K., *Phys. Rev. E* 81: 026309 (2010).
[16] Valiev D., Bychkov V., Akkerman V., Eriksson L.-E., *Phys. Rev. E* 80: 036317 (2009).
[17] Bychkov V., Akkerman V., Valiev D., Law C.K., *Combust. Flame* 157: 2008 (2010).